Electronic Supplementary Material (ESI) for Journal of Materials Chemistry A.

Supporting Information

Fluorosulfide $La_{2.7}Ba_{6.3}F_{8.7}S_6$ with Double-Layer Honeycomb Structure Enabling Fluoride-Ion Conduction

Shintaro Tachibana[a], Chengchao Zhong*[a], Takeshi Tojigamori[b], Hidenori Miki[b], Toshiyuki Matsunaga[c] and Yuki Orikasa*[a]

[a] Graduate School of Life Sciences, Ritsumeikan University, 1-1-1 Noji-higashi, Kusatsu, Shiga 525-8577, Japan.

[b] Advanced Material Engineering Division., Toyota Motor Corporation, 1200 Mishuku, Susono, Shizuoka 410-1193, Japan.

[c] Graduate School of Human and Environmental Studies, Kyoto University, Yoshida-nihonmatsu-cho, Sakyo, Kyoto, 606-8501, Japan.

* Yuki Orikasa (orikasa@fc.ritsumei.ac.jp), Chengchao Zhong(zcc.sschem@gmail.com)

S.1: Refined structural parameters of $La_{2.7}Ba_{6.3}F_{8.7}S_6$ and $La_{2.16}Ba_{6.3}Ca_{0.54}F_{8.16}S_6$

Table S1. Refined structural parameters of $La_3Ba_6F_9S_6$ obtained by Rietveld refinement of X-ray diffraction data.

Atom	Wyckoff	*g*	*x*	*y*	*z*	*U* / Å^3	BVS
La1	3 *b*	1	0	0	1/2	0.011(13)	+2.03
Ba1	6 *c*	1	0	0	0.28286(9)	0.014(10)	+2.33
S1	6 *c*	1	0	0	0.1146(4)	0.028(4)	−1.78
F1	6 *c*	1	0	0	0.3673(9)	0.07(10)	−1.24
F2	3 *a*	1	0	0	0	0.14(2)	−0.64

Unit cell: trigonal *R*-3(148); $a = 4.38603(6)$ Å, $c = 32.4193(7)$ Å

$R_{wp} = 11.01\%$, $R_p = 6.23\%$, goodness of fit $S = 1.19$

Table S2. Refined structural parameters of $La_{2.7}Ba_{6.3}F_{8.7}S_6$ obtained by Rietveld refinement of X-ray diffraction data. In order to avoid including errors for anions, the fluorine site occupancies were fixed.

Atom	Wyckoff	*g*	*x*	*y*	*z*	*U* / Å^3
La1	3 *b*	0.387(5)	0	0	1/2	0.010(13)
Ba1	3 *b*	0.613(5)	0	0	= *z*(La1)	= *U*(La1)
La2	6 *c*	0.257(9)	0	0	0.28286(9)	0.015(10)
Ba2	6 *c*	0.743(9)	0	0	= *z*(La2)	= *U*(La2)
S1	6 *c*	1	0	0	0.1147(4)	0.029(4)
F1	6 *c*	1	0	0	0.3672(9)	0.07(10)
F2	3 *a*	0.9	0	0	0	0.10(2)

Unit cell: trigonal *R*-3(148); $a = 4.38602(6)$ Å, $c = 32.4192(7)$ Å

$R_{wp} = 10.97\%$, $R_p = 6.19\%$, goodness of fit $S = 1.18$

Table S3. Refined structural parameters of $La_{2.7}Ba_{6.3}F_{8.7}S_6$ obtained by Rietveld refinement of neutron diffraction data.

Atom	Wyckoff	*g*	*x*	*y*	*z*	*U* / Å^2
La1	3 *b*	0.457(2)	0	0	1/2	0.0118(10)
Ba1	3 *b*	0.543(2)	0	0	= *z*(La1)	= *U*(La1)
La2	6 *c*	0.2216(10)	0	0	0.282748(5)	0.01326(9)
Ba2	6 *c*	0.7784(10)	0	0	= *z*(La2)	= *U*(La2)
S1	6 *c*	1	0	0	0.114504(14)	0.03284(9)
F1	6 *c*	0.9859(7)	0	0	0.366128(9)	0.04877(9)
F2	3 *a*	0.9281(14)	0	0	0	0.1157(2)

Atom	U_{11} / Å^2	U_{22} / Å^2	U_{33} / Å^2	U_{12} / Å^2	U_{13} / Å^2	U_{23} / Å^2
La1	0.007843(11)	0.007843(11)	0.01962(2)	0.00392(7)	0	0
Ba1	= U_{11}(La1)	= U_{22}(La1)	= U_{33}(La1)	= U_{12}(La1)	= U_{13}(La1)	= U_{23}(La1)
La2	0.01489(8)	0.01489(8)	0.0100(12)	0.00745(4)	0	0
Ba2	= U_{11}(La2)	= U_{22}(La2)	= U_{33}(La2)	= U_{12}(La2)	= U_{13}(La2)	= U_{23}(La2)
S1	0.0310(12)	0.0310(12)	0.0365(3)	0.01549(8)	0	0
F1	0.0505(12)	0.0505(12)	0.0453(18)	0.02525(7)	0	0
F2	0.1130(3)	0.1130(3)	0.1211(9)	0.0565(17)	0	0

Unit cell: trigonal *R*-3(148); *a* = 4.3870457 (13) Å, *c* = 32.43296(3) Å

R_{wp} = 8.84%, R_e = 1.41%, goodness of fit *S* = 6.25

Table S4. Refined structural parameters of $La_{2.16}Ba_{6.3}Ca_{0.54}F_{8.16}S_6$ obtained by Rietveld refinement of neutron diffraction data.

Atom	Wyckoff	*g*	*x*	*y*	*z*	*U* / Å^2
La1	3 *b*	0.4612(17)	0	0	1/2	0.01426(9)
Ba1	3 *b*	0.5032(9)	0	0	= *z*(La1)	= *U*(La1)
Ca1	3 *b*	0.0356(8)	0	0	= *z*(La1)	= *U*(La1)
La2	6 *c*	0.1293(8)	0	0	0.282977(5)	0.01464(8)
Ba2	6 *c*	0.7984(4)	0	0	= *z*(La2)	= *U*(La2)
Ca2	6 *c*	0.0722(4)	0	0	= *z*(La2)	= *U*(La2)
S1	6 *c*	1	0	0	0.114960(11)	0.02684(9)
F1	6 *c*	0.9987(7)	0	0	0.365078(7)	0.05043(9)
F2	3 *a*	0.7225(15)	0	0	0	0.07977(3)

Atom	U_{11} / Å^2	U_{22} / Å^2	U_{33} / Å^2	U_{12} / Å^2	U_{13} / Å^2	U_{23} / Å^2
La1	0.0118(11)	0.0118(11)	0.0192(2)	0.00592(7)	0	0
Ba1	= U_{11}(La1)	= U_{22}(La1)	= U_{33}(La1)	= U_{12}(La1)	= U_{13}(La1)	= U_{23}(La1)
Ca1	= U_{11}(La1)	= U_{22}(La1)	= U_{33}(La1)	= U_{12}(La1)	= U_{13}(La1)	= U_{23}(La1)
La2	0.01711(8)	0.01711(8)	0.0097(11)	0.00856(4)	0	0
Ba2	= U_{11}(La2)	= U_{22}(La2)	= U_{33}(La2)	= U_{12}(La2)	= U_{13}(La2)	= U_{23}(La2)
Ca2	= U_{11}(La2)	= U_{22}(La2)	= U_{33}(La2)	= U_{12}(La2)	= U_{13}(La2)	= U_{23}(La2)
S1	0.0289(11)	0.0289(11)	0.0227(2)	0.01444(6)	0	0
F1	0.0566(11)	0.0566(11)	0.0381(18)	0.02830(6)	0	0
F2	0.0748(3)	0.0748(3)	0.0897(5)	0.0374(18)	0	0

Unit cell: trigonal *R*-3(148); a = 4.3640735(13) Å, c = 32.34269(3) Å

R_{wp} = 5.55%, R_e = 1.32%, goodness of fit S = 4.20

S. 2: Crystal structure analysis of $La_{2.7}Ba_{6.3}F_{8.7}S_6$

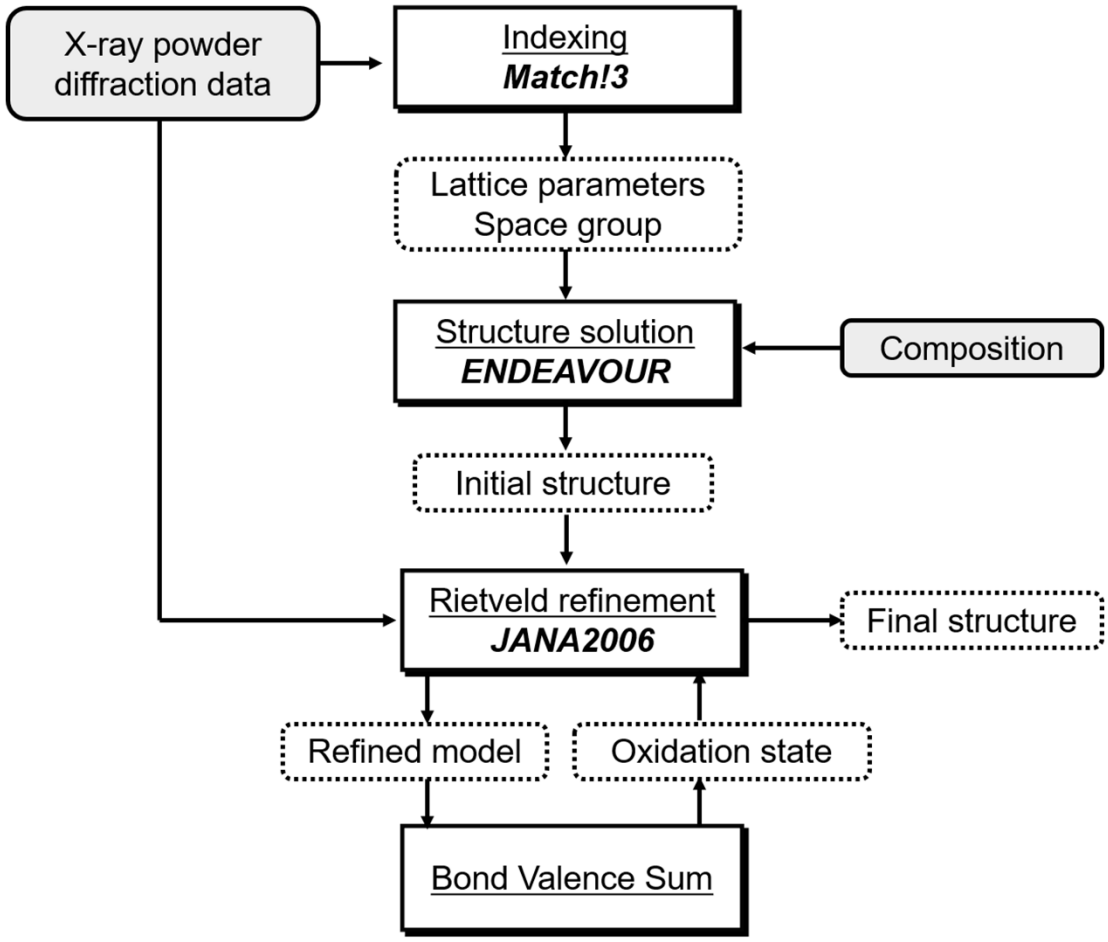

Figure S1. Flow-chart of structural determination for powder diffraction. The square includes the structural method with underline and program name written italic. The dotted circle indicates the structural parameters, whereas the circle with grey background indicates the experimental data.

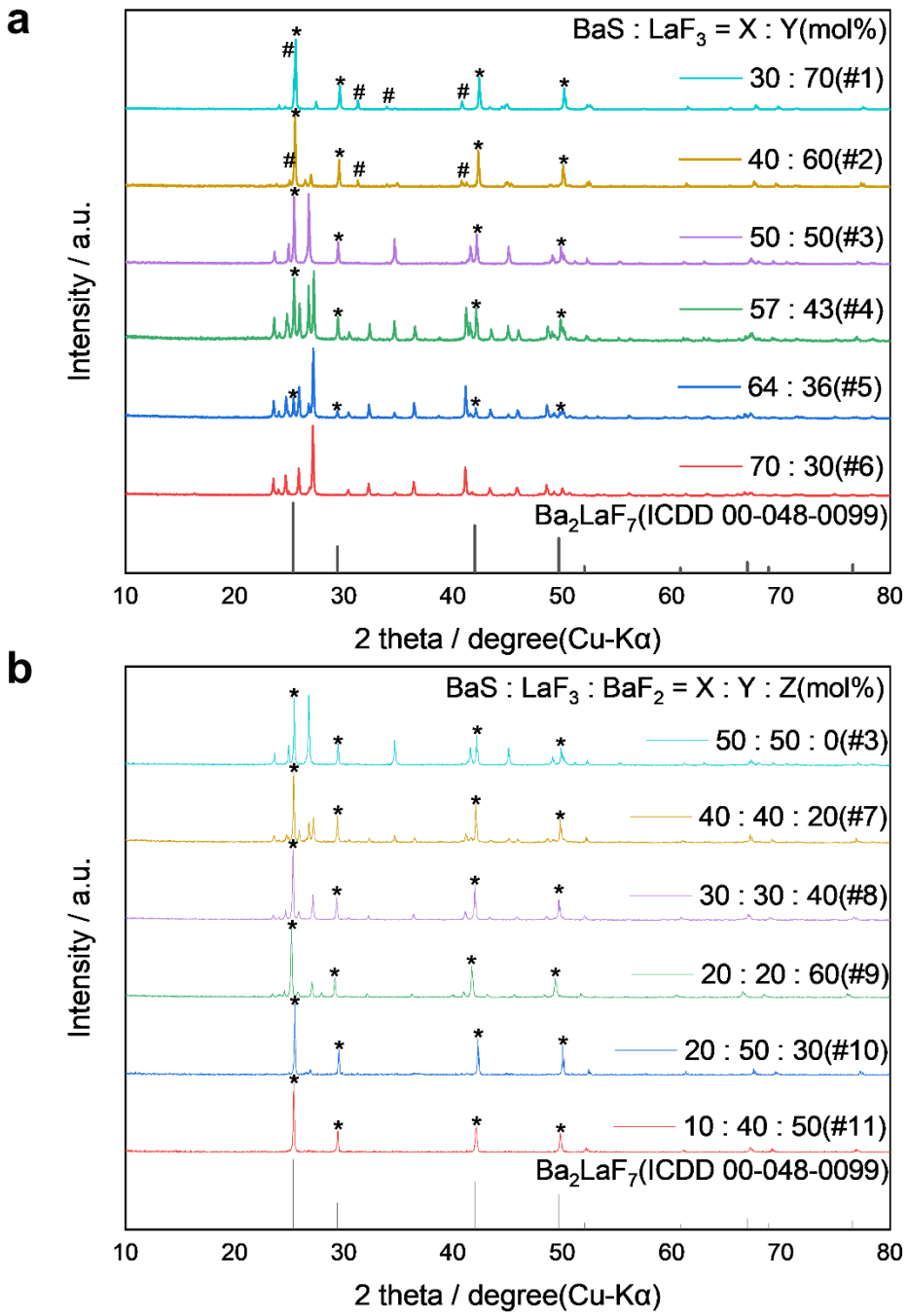

Figure S2. XRD patterns (λ = 1.5418 Å) of the synthesized compounds and reference data for Ba_2LaF_7(00-048-0099)[1] from International Centre for Diffraction Data(ICDD). The sharps(#) and asterisks(*) indicate LaFS and Ba_2LaF_7 phases, respectively.

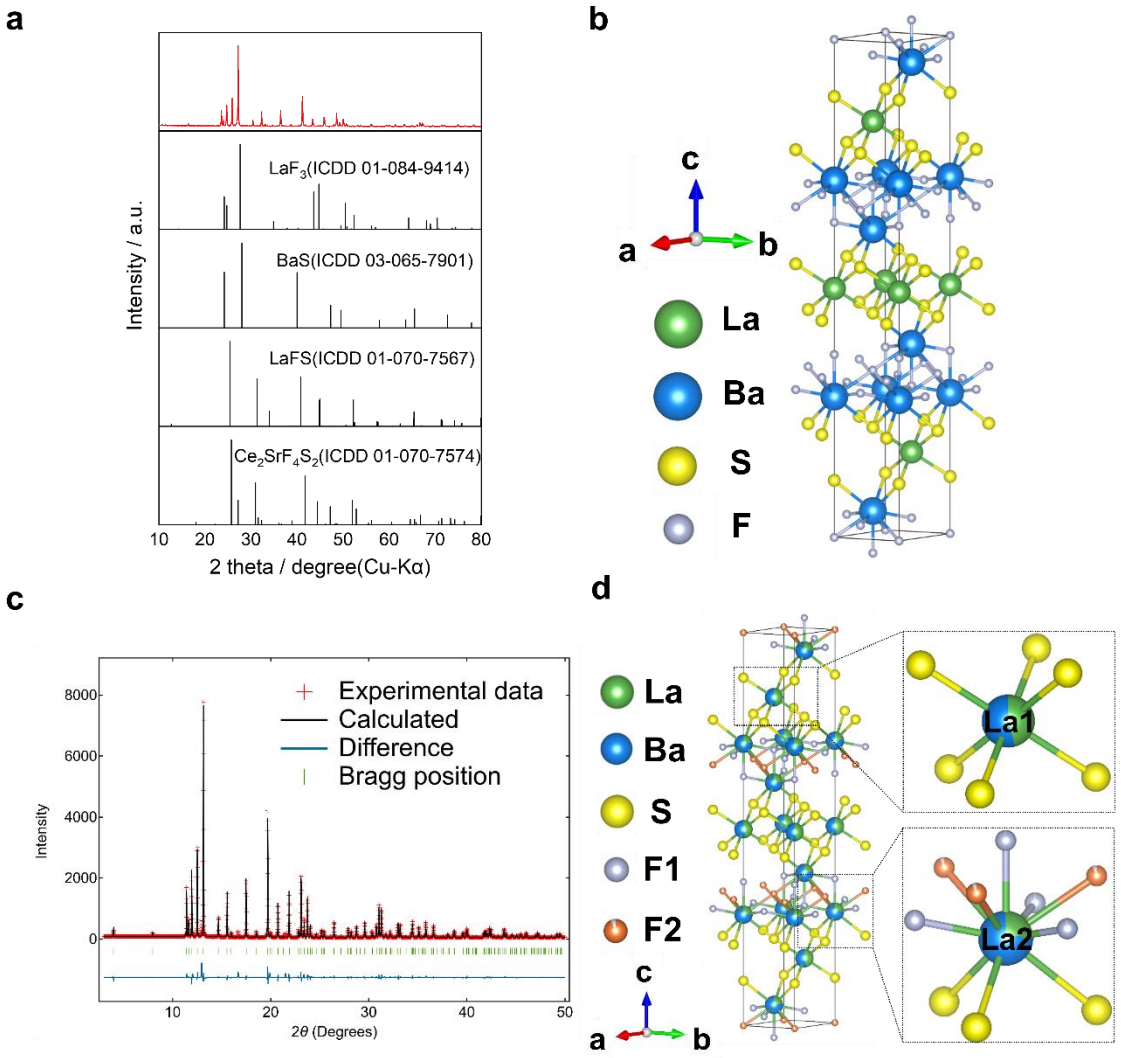

Figure S3. (a) XRD patterns (λ = 1.5418 Å) of the synthesized compound weighted the molar ratio BaS:LaF_3 = 70:30 and reference data for LaF_3(01-084-9414)[2], BaS(03-065-7901)[3], LaFS(01-070-7567)[4], $Ce_2SrF_4S_2$(01-070-7574)[4] from International Centre for Diffraction Data(ICDD). **(b)** Refined crystal structure of $La_3Ba_6F_9S_6$. (**c**) Rietveld patterns of $La_{2.7}Ba_{6.3}F_{8.7}S_6$. Red plus, black lines, and blue lines denote observed, calculated, and difference, respectively. Green ticks represent the Bragg position of $La_{2.7}Ba_{6.3}F_{8.7}S_6$. (**d**) Refined crystal structure of $La_{2.7}Ba_{6.3}F_{8.7}S_6$ (space group: *R*-3). The unit cell is shown by the solid lines.

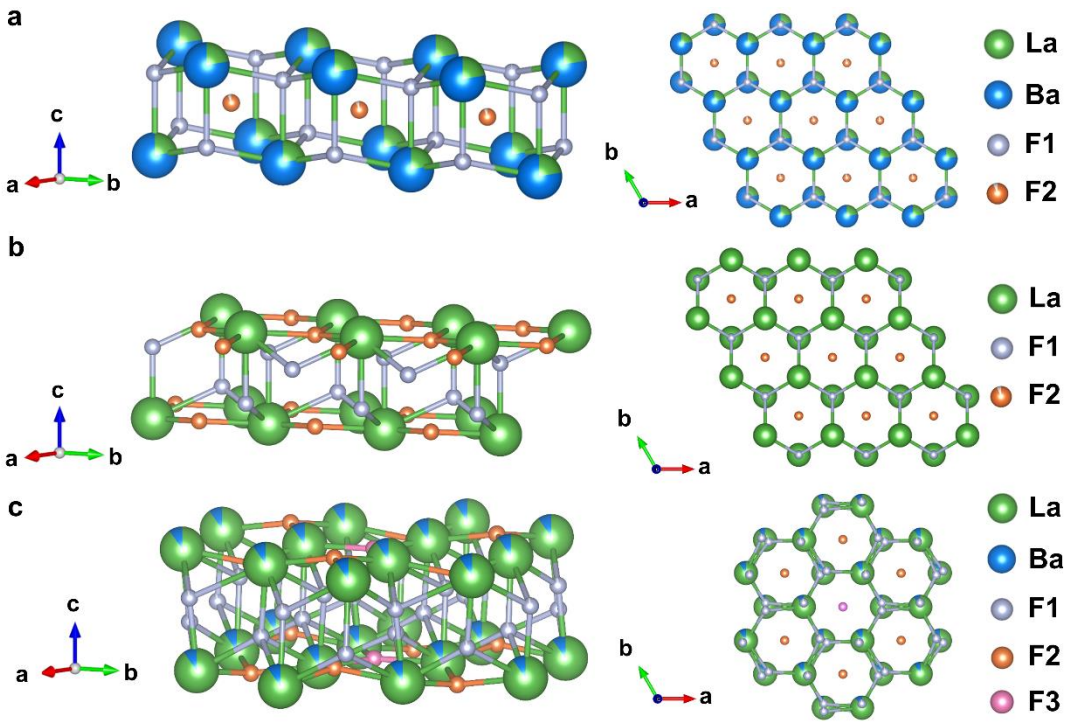

Figure S4. Enlarged view near double honeycomb fluoride ion layers and the view along *ab*-plane. of (a) $La_{2.7}Ba_{6.3}F_{8.7}S_6$, (b) LaF_2I[5] and (c) $La_{0.9}Ba_{0.1}F_{2.9}$[6]. All the compounds form the fluoride-ion conduction layers with a honeycomb structure along *ab*-plane.

S. 3: Fluoride ion conductivity and electrochemical window of $La_{2.7}Ba_{6.3}F_{8.7}S_6$

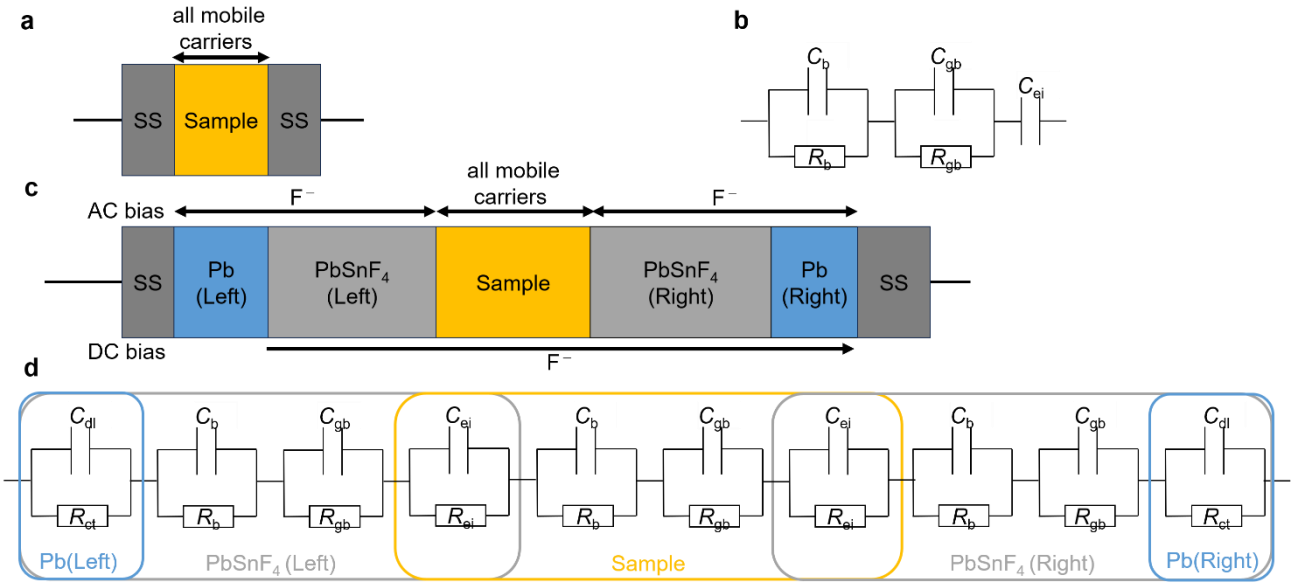

Figure S5. Schematic illustration of the cell and equivalent circuit for the evaluation of the ionic conductivity of the synthesized compounds and the confirmation of conduction carrier species of the synthesized sample. (a) Schematic illustration of the symmetric cell for the evaluation of the ionic conductivity of the sample by AC impedance and (b) the equivalent circuit model of the symmetric cell. The model is composed by the electrolyte component (R_b : bulk resistance, C_b : bulk capacitance, R_{gb} : grain boundary resistance, C_{gb} : grain boundary capacitance) based on the ion conduction in the solid and the electrode interface resistance (C_{ei}) due to the polarization effects at the electrode/electrolyte interfaces. (c) Schematic illustration of the blocking cell for the confirmation of the dominant carrier species of the sample by AC impedance and DC conductivity measurements. (d) The equivalent circuit model of the blocking cell. The model consists of electrolyte (sample and two $PbSnF_4$ on both sides) components, the resistance component (R_{ei} : electrode interface resistance, C_{ei} : electrode interface capacitance) between electrolytes ($PbSnF_4$/sample), and the resistance component (R_{ct} : charge transfer resistance, C_{dl} : double layer capacitance) due to the decomposition of $PbSnF_4$ by fluoride ion migration between Pb electrode and $PbSnF_4$.

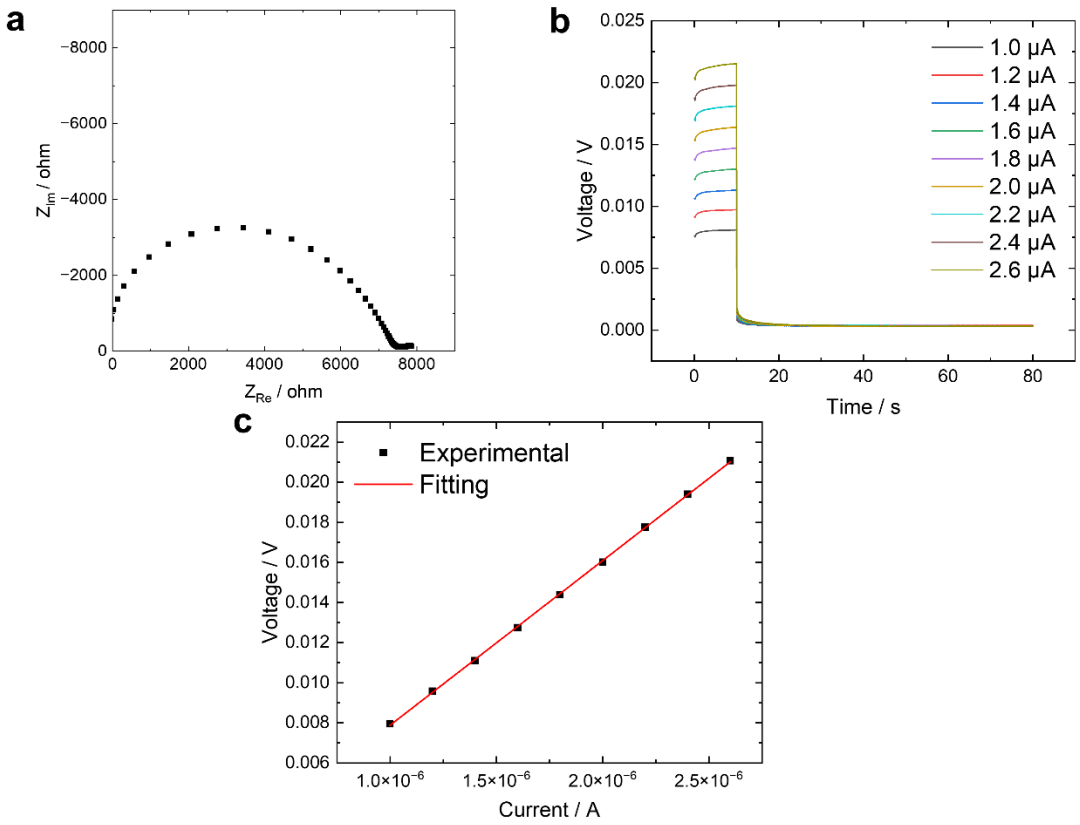

Figure S6. Confirmation of conduction carrier of $La_{2.7}Ba_{6.3}F_{8.7}S_6$. **(a)**Nyquist plots from AC impedance measurement and **(b)** Voltage-time profile of SS|Pb|$PbSnF_4$|$La_{2.7}Ba_{6.3}F_{8.7}S_6$|$PbSnF_4$|Pb|SS blocking cell at 423 K. **(c)** *I-V* plots for data obtained 2 s after applying current. Since $PbSnF_4$ is an almost pure fluoride ion conductor, the cell conducts only fluoride ions under DC method, while all mobile ions in the cell conduct under AC impedance measurements[7]. The resistance value of SS|Pb|$PbSnF_4$|$La_{2.7}Ba_{6.3}F_{8.7}S_6$|$PbSnF_4$|Pb|SS symmetrical blocking cell observed in the AC impedance measurements is 7552 ohm, whereas the resistance value of the same cell in observed in the DC method is 8205 ohm. The almost similar resistance of the AC impedance measurement and that of DC method indicates fluoride ion as conduction carrier of $La_{2.7}Ba_{6.3}F_{8.7}S_6$. However, the absolute resistance value in this measurement is smaller than that observed in Fig. 3. This is probably due to $PbSnF_4$ has infiltrated the gaps around the pellet, reducing the effective thickness. Further investigation of this method is required.

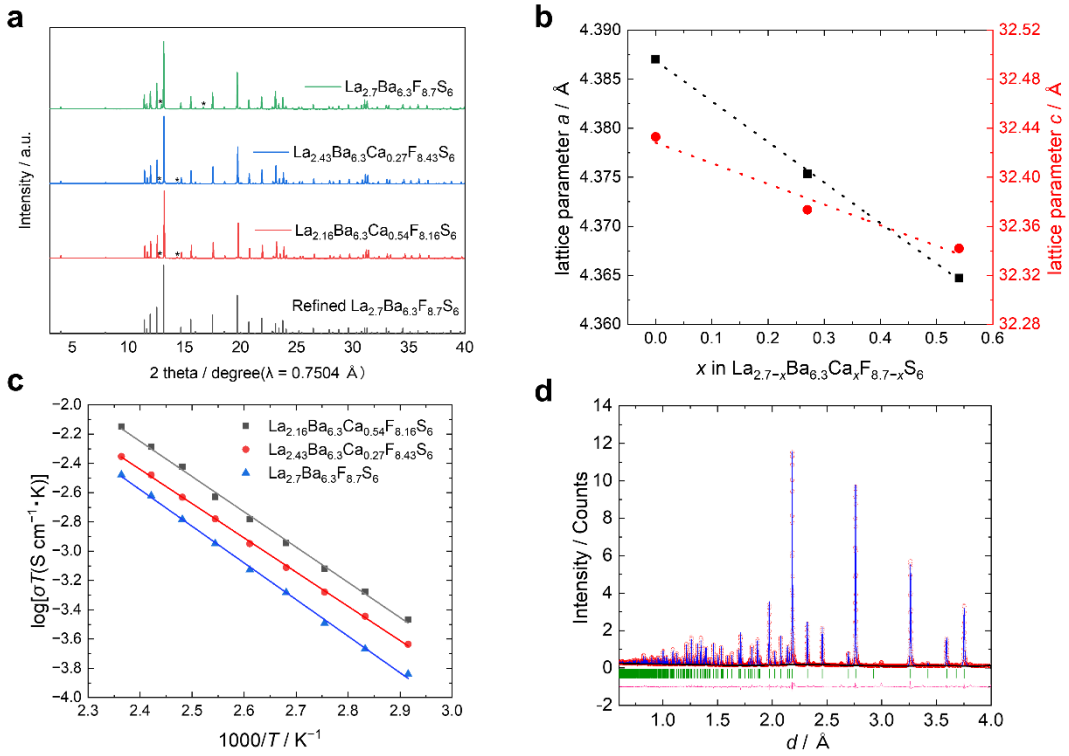

Figure S7. (a) X-ray diffraction patterns of the synthesized $La_{2.7-x}Ba_{6.3}Ca_xF_{8.7-x}S_6$ (x = 0, 0.27, 0.54) and diffraction peaks of the refined $La_{2.7}Ba_{6.3}F_{8.7}S_6$ (λ = 0.7504 Å). The asterisks (*) represent the peaks of impurities. **(b)** Composition dependence of lattice parameters for $La_{2.7-x}Ba_{6.3}Ca_xF_{8.7-x}S_6$ (x = 0, 0.27, 0.54). From $La_{2.7}Ba_{6.3}F_{8.7}S_6$ to $La_{2.16}Ba_{6.3}Ca_{0.54}F_{8.16}S_6$, the lattice parameters of a and c gradually decrease in line with Vegard's law. The decreased lattice volume is attributed to the varying ionic radii of lanthanum (103 pm) and calcium (100 pm) in the $La_{2.7-x}Ba_{6.3}Ca_xF_{8.7-x}S_6$ phase. **(c)** Arrhenius plot of the sintered $La_{2.7-x}Ba_{6.3}Ca_xF_{8.7-x}S_6$. **(d)** Neutron Rietveld refinement of $La_{2.16}Ba_{6.3}Ca_{0.54}F_{8.16}S_6$. Red circle, blue line and pink line stands for the observed, calculated, and difference, respectively. Green ticks represent the Bragg position of $La_{2.16}Ba_{6.3}Ca_{0.54}F_{8.16}S_6$.

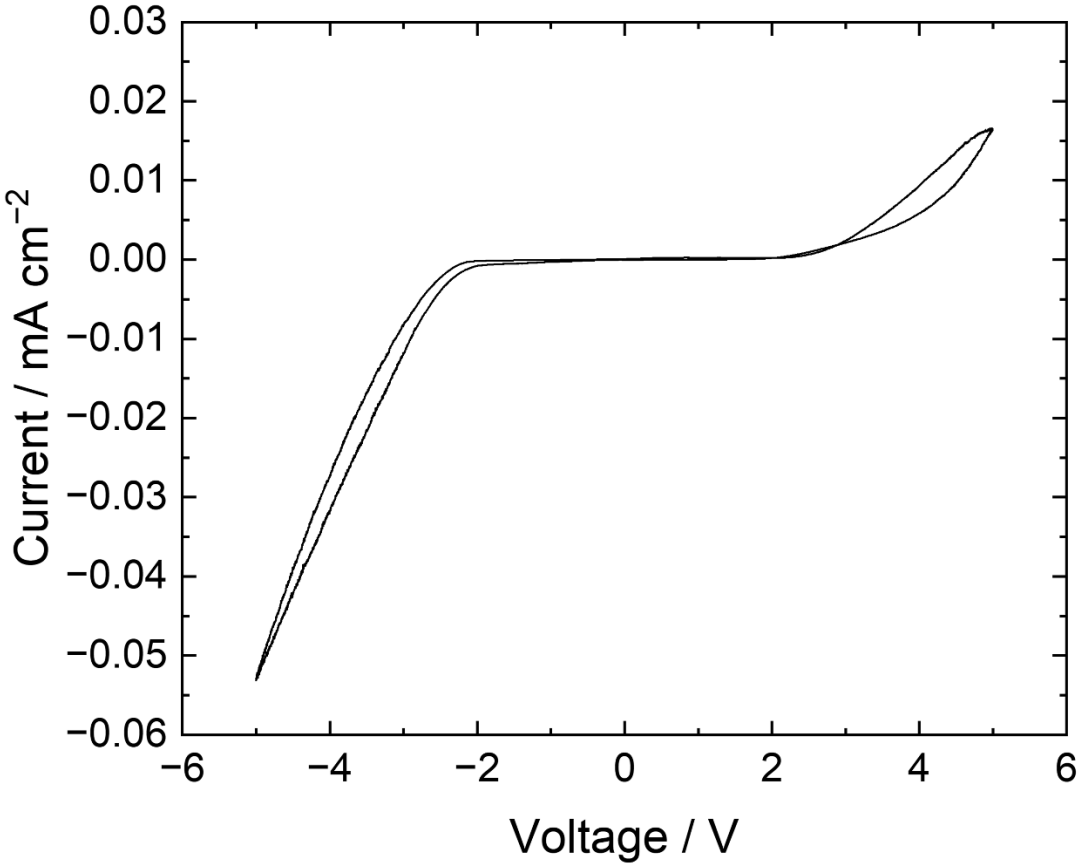

Figure S8. Cyclic voltammogram of the SS|Pt|$La_{2.7}Ba_{6.3}F_{8.7}S_6$|Pb/$PbF_2$|SS cell at 423 K. The electrochemical potential window of $La_{2.7}Ba_{6.3}F_{8.7}S_6$ exceeds 4.0 V.

S. 4: Mechanism of fluoride ion conduction

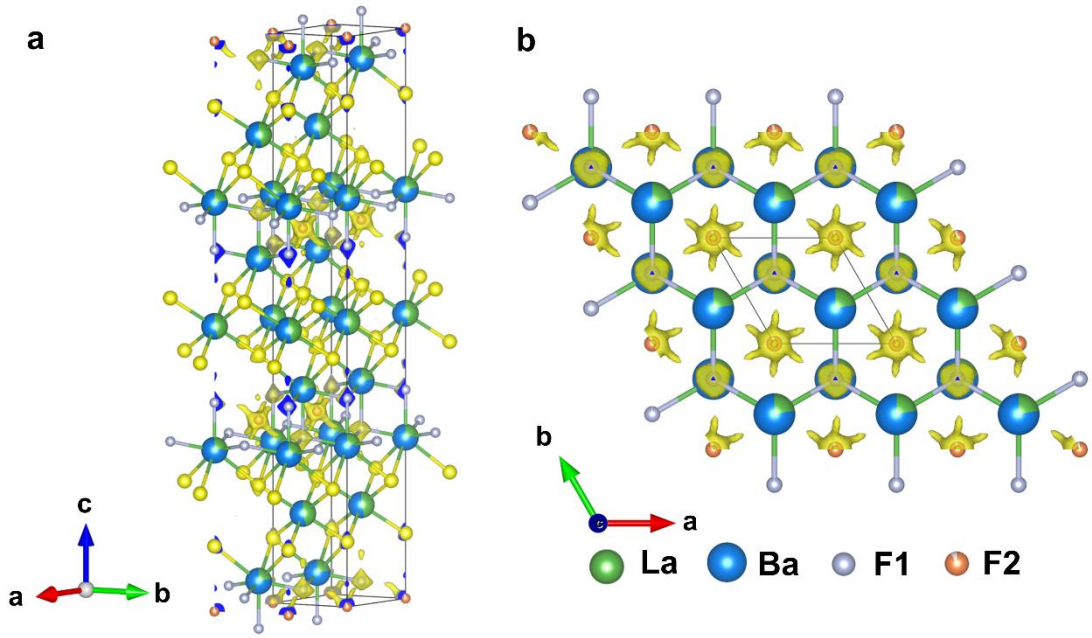

Figure S9. (a) Three-dimensional nuclear density distributions calculated by maximum-entropy method using neutron diffraction data for $La_{2.7}Ba_{6.3}F_{8.7}S_6$ at 1.0 fm $Å^{-3}$. (b) Enlarged view of the nuclear density distributions along *ab*-plane.

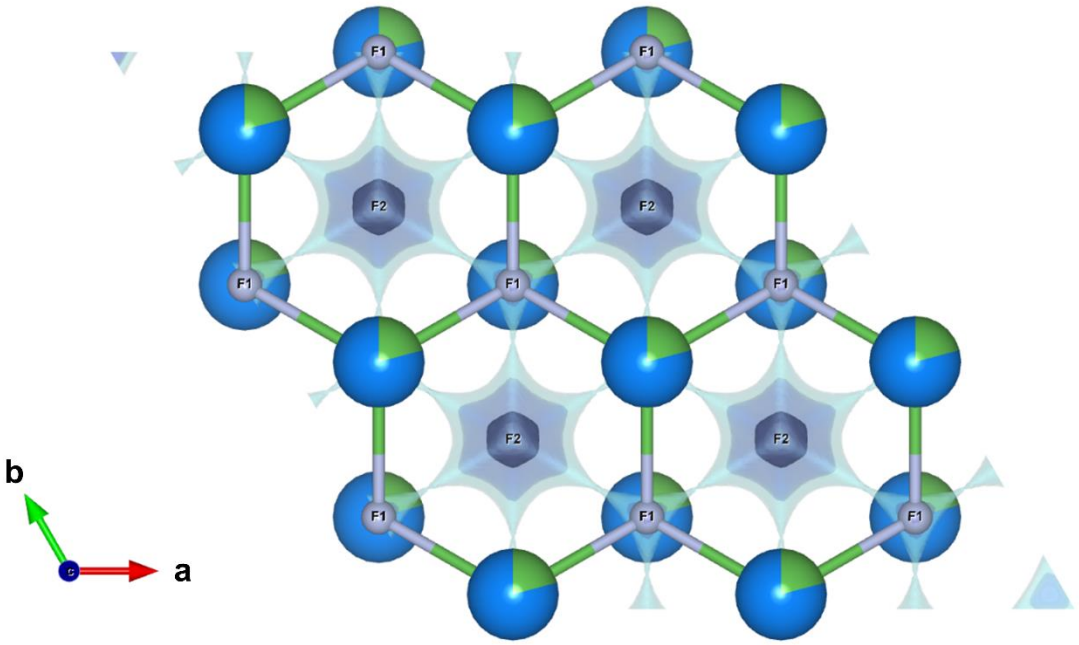

Figure S10. Fluoride ion conduction pathway calculated by BV-based energy calculation of $La_{2.7}Ba_{6.3}F_{8.7}S_6$.

References

1. U. R. K. Rao, A. K. Tyagi, K. V. Muralidharan and R. M. Iyer, *J. Mater. Sci. Lett.*, 1992, **11**, 435-436.
2. N. B. Bolotina, T. S. Chernaya, A. I. Kalyukanov, I. A. Verin, N. I. Sorokin, L. E. Fykin, N. N. Isakova and B. P. Sobolev, *Crystallogr. Rep.*, 2015, **60**, 346-360.
3. J. Flahaut, L. Domange and M. Patrie, *Bull. Soc. Chim. Fr*, 1962, 2048-2054.
4. A. Demourgues, A. Tressaud, H. Laronze and P. Macaudière, *J. Alloys Compd.*, 2001, **323-324**, 223-230.
5. D. Kato, P. Song, H. Ubukata, H. Taguro, C. Tassel, K. Miyazaki, T. Abe, K. Nakano, K. Hongo, R. Maezono and H. Kageyama, *Angew. Chem. Int. Ed. Engl.*, 2023, **62**, e202301416.
6. T. S. Chernaya, I. A. Verin, O. N. Khrykina and N. B. Bolotina, *Crystallogr. Rep.*, 2018, **63**, 45-51.
7. K. Motohashi, Y. Matsukawa, T. Nakamura, Y. Kimura, N. Kuwata, Y. Uchimoto and K. Amezawa, *Sci. Rep.*, 2022, **12**, 5955.